The Plant Cell, Vol. 3, 1327–1336, December 1991 © 1991 American Society of Plant Physiologists

Allelic Interactions at the *nivea* Locus of Antirrhinum

Joachim Bollmann,[1] Rosemary Carpenter, and Enrico S. Coen[2]

John Innes Institute, John Innes Centre, Colney Lane, Norwich NR4 7UH, United Kingdom

Most null alleles at the *nivea* (*niv*) locus are recessive to *Niv*$^+$ and, when homozygous, give white flowers rather than the red of the wild type. In contrast, the *niv-571* allele is semidominant; although it gives white flowers when homozygous, very pale flowers result when this allele is heterozygous with *Niv*$^+$. We showed that in heterozygotes, *niv-571* acts in *trans* to inhibit expression of its *Niv*$^+$ homolog 25-fold to 50-fold. The inhibition is reversible after meiosis and partially reversible somatically. The *niv-571* allele carries a transposable element Tam3 insertion and three truncated copies of the *niv* gene, one copy being in inverse orientation. Analysis of two further *niv* alleles, *niv-572* and *niv-527*, showed that excision of Tam3 from *niv-571* does not affect the ability of the allele to repress *Niv*$^+$ and that one truncated *niv* copy alone is insufficient to confer semidominance. The detailed structures of various semidominant *niv* alleles suggest that their effects in *trans* are not readily explained by production of antisense RNA but are more easily reconciled with a direct recognition/interaction between homologous genes, reminiscent of cosuppression and transvection phenomena described in other systems.

INTRODUCTION

In diploid organisms, both alleles at a locus are normally expressed independently of each other. There are exceptions to this rule, however. In allelic exclusion, one of the two immunoglobulin alleles is not expressed. Dosage compensation in female mammalian cells results in most alleles on one X chromosome being transcriptionally silent (Davies, 1991). In Drosophila, certain alleles can interact with each other if their chromosomal position allows for synapsis; this is a phenomenon known as transvection (Wu and Goldberg, 1989; Bickel and Pirrotta, 1990; Geyer et al., 1990). To gain further insight into the possible mechanisms underlying allelic interactions, we have studied an example at the *nivea* (*niv*) locus in Antirrhinum.

The *niv* gene encodes an enzyme, chalcone synthase, required for an early step in anthocyanin pigment biosynthesis. Many *niv* alleles have been obtained as a consequence of transposable element activity (Carpenter et al., 1987; Martin et al., 1988; Sommer et al., 1988; Martin and Lister, 1989). Most of these are recessive null alleles, giving albino flowers in contrast to full red flowers of the wild type. One of these alleles, *niv-525*, however, is semidominant to the wild type and appears to repress expression of its *Niv*$^+$ wild-type homolog in *Niv*$^+$/*niv-525* heterozygotes (Coen and Carpenter, 1988). The only structural difference between *niv-525* and *Niv*$^+$ is a 207-bp inverted duplication comprising 62 bp of a promoter region and 145 bp of a transcribed region. The structure of this allele led to several possible models to explain the semidominance (Coen and Carpenter, 1988). One proposed a direct interaction between *niv-525* and *Niv*$^+$ alleles, perhaps analogous to the allelic interactions underlying certain transvection phenomena in Drosophila, already cited above. Another model invoked the production of antisense RNA resulting from transcription of the inverted region of the *niv* gene. Antisense RNA might inhibit expression of *Niv*$^+$ in *trans* by formation of RNA-RNA hybrids.

Here we describe a further semidominant allele of the *niv* locus, *niv-571*, which inhibits *Niv*$^+$ expression even more effectively than does *niv-525*. For comparison, the *niv-525*/*niv-525* and *Niv*$^+$/*niv-525* phenotypes are shown in Figure 1A. The phenotype of *niv-571*/*Niv*$^+$ heterozygotes is comparable to that of the *niv-525* homozygotes (Figure 1A). These flowers should be compared with those of a recessive null mutation such as *niv-527*; homozygous *niv-527* plants have white flowers and *Niv*$^+$/*niv-527* plants have full red flowers (Figure 1A). This is presumably because a single copy of the *Niv*$^+$ allele produces enough RNA to allow wild-type levels of anthocyanin to be made (Sommer et al., 1988). We show here that the structures of *niv-571* and related alleles, *niv-572* and *niv-527*, are not easily reconciled with the involvement of antisense RNA in semidominance but are consistent with a direct physical interaction or recognition between alleles.

[1] Current address: Bundesministerium für Ernährung, Landwirtschaft und Forsten, Rochusstrasse 1, D-5300 Bonn, Federal Republic of Germany.

[2] To whom correspondence should be addressed.

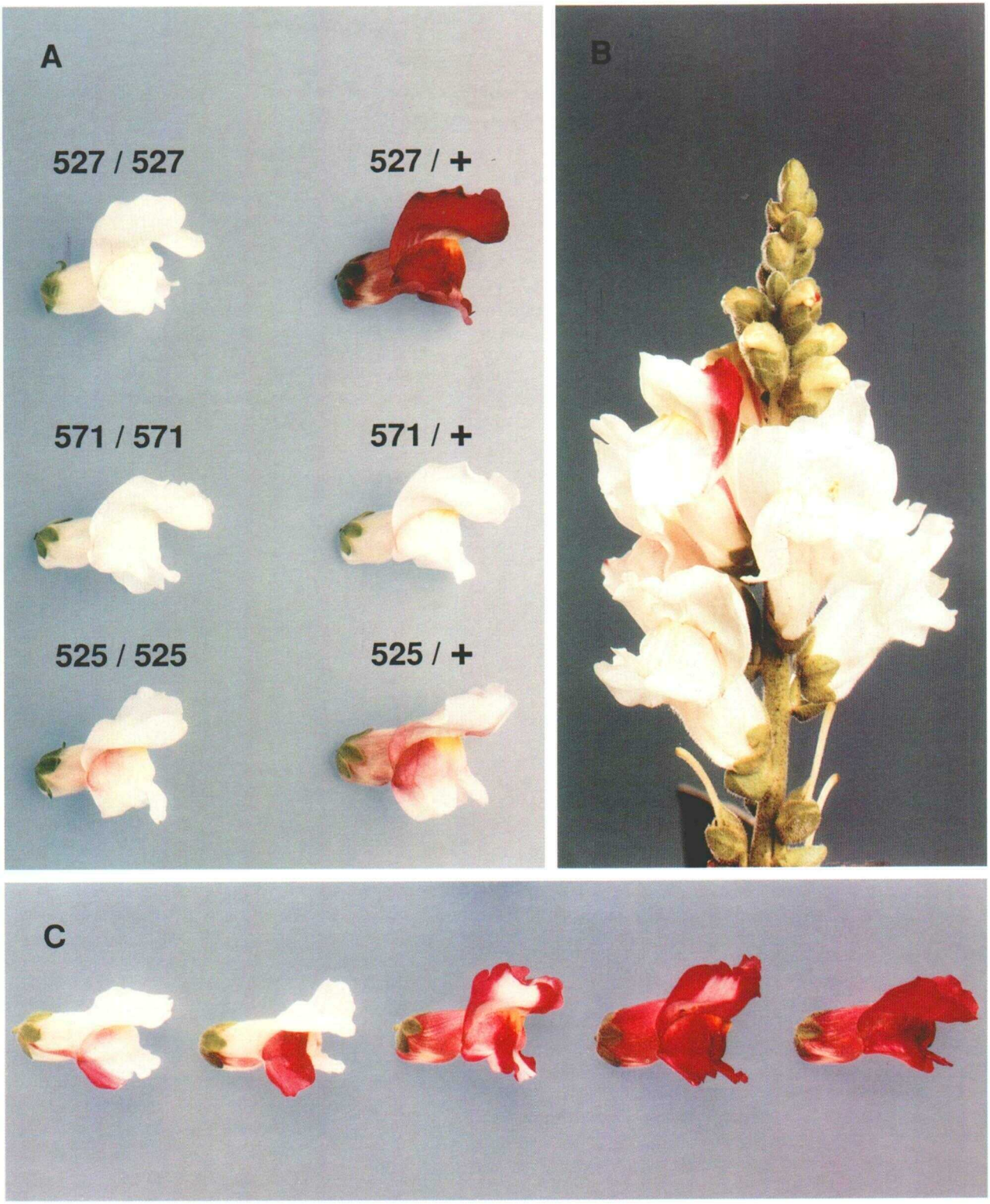

Figure 1. Phenotypes Conferred by Several *niv* Alleles of Antirrhinum.

(A) Flowers and their respective genotypes.

RESULTS

niv-571 Reduces Expression of *Niv*$^+$ in *trans*

The *niv-98* allele gives pale red flowers with full red sites of pigmentation superimposed because of genetic instability caused by the presence of the transposable element Tam3 in the promoter of the *niv* gene (Sommer et al., 1985). In the progeny of *niv-98* homozygotes, a single plant with very pale flowers was obtained. Because most *niv* alleles are recessive, this very pale phenotype suggested either that a mutation in both alleles had occurred or that there had been a semidominant mutation in one allele. Of the progeny obtained from selfing of the very pale plant, one-quarter had a typical *niv-98/niv-98* phenotype, half had very pale flowers similar to their parent, and one-quarter had white flowers. This indicated that a semidominant allele, subsequently called *niv-571*, was responsible for the new phenotype. One of the white-flowered plants was self-pollinated to give rise to a true-breeding, white-flowered stock, JI 571. When this stock was crossed with full red wild-type plants, the heterozygous progeny had flowers with very little coloration and a specific spatial pattern of pigment distribution: anthocyanin was mainly located at the edges of the lower lips (Figure 1A). The total amount of anthocyanin in heterozygous flowers was about 2% of that in the homozygous wild type. Occasionally, heterozygotes had a few flowers with red sectors, sometimes with fuzzy or diffuse boundaries (Figure 1B), and very rarely whole flowers with a new spatial pattern of pigment distribution; the degree and pattern of pigmentation varied between individual reversion events (Figure 1C).

RNA gel blots of flower RNA probed with a *niv* cDNA clone detected no *niv* transcript in RNA from *niv-571* homozygotes, as shown in Figure 2A, and detected 1% to 2% of the transcript in *niv-571/Niv*$^+$ heterozygotes compared with *Niv*$^+$*/Niv*$^+$ homozygotes (Figure 2B). Assuming that one dose of a *Niv*$^+$ allele contributed 50% of the transcript observed in *Niv*$^+$*/Niv*$^+$ flowers, the level of transcript detected in *niv-571/Niv*$^+$ flowers implied that the amount of transcript from the *Niv*$^+$ allele was reduced 25- to 50-fold. The expression of *pallida*, a gene involved in a later step in anthocyanin biosynthesis (dihydroflavonol reductase, Coen et al., 1986; Almeida et al., 1989), was unaffected by *niv-571* (Figure 2C), indicating that the repression was specific to *Niv*$^+$.

The *trans* inhibition of *Niv*$^+$ by *niv-571* is similar to that observed for another *niv* mutation, *niv-525* (Coen and Carpenter, 1988). However, *niv-525* gives a fourfold to fivefold inhibition of *Niv*$^+$ compared with the 25- to 50-fold inhibition by *niv-571*.

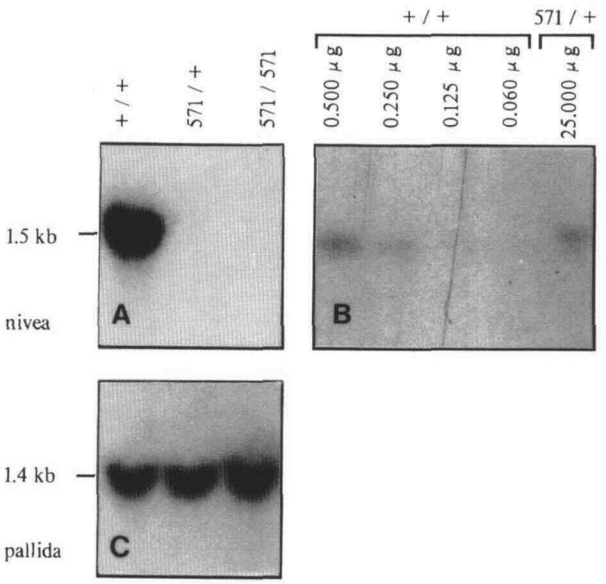

Figure 2. Transcript Analysis of *niv-571*.

(A) Gel blot hybridization with total RNA (25 μg) from flowers probed with the 1.0-kb EcoRI fragment of the *niv* cDNA clone pAm10 (Sommer and Saedler, 1986).
(B) Gel blot hybridization with varying amounts of total RNA from flowers probed with the same *niv* probe as in **(A)**.
(C) RNA as in **(A)** probed with the 4.3-kb HindIII fragment from the *pallida* genomic clone pJAM501.

Structure of *niv-571*

The structure of the *niv-571* allele was investigated by DNA gel blot hybridization, as shown in Figure 3, to Am3, a cloned 5.7-kb EcoRI fragment of the *niv* locus containing most of the 5′ *niv* coding region (1.9 kb) together with 3.8 kb of upstream sequences (Sommer and Saedler, 1986). The position of Am3 on the restriction map of the *niv* gene is given in Figure 4. As expected, Am3 detected a 5.7-kb EcoRI fragment in wild-type plants (Figure 3A). The progenitor of *niv-571*, *niv-98*, carries the 3.6-kb transposable element Tam3 in the *niv* promoter and, because Tam3 carries no EcoRI site, produced an EcoRI fragment of 9.3 kb. In *niv-571*, two fragments hybridized at 7.5 kb and 2.2 kb. In F_2 populations of crosses between *niv-571* and wild type, all plants with white or palely patterned flowers carried both the 7.5- and 2.2-kb fragments (50 plants analyzed). This showed that the two fragments were linked and confirmed that the very pale or white-flowered phenotype was conferred by an alteration at the *niv* locus.

Figure 1. (continued).

(B) Spike from *Niv*$^+$*/niv-571* plant showing flowers with red sectors.
(C) Flowers from different *Niv*$^+$*/niv-571* plants showing independent somatic reversion events.

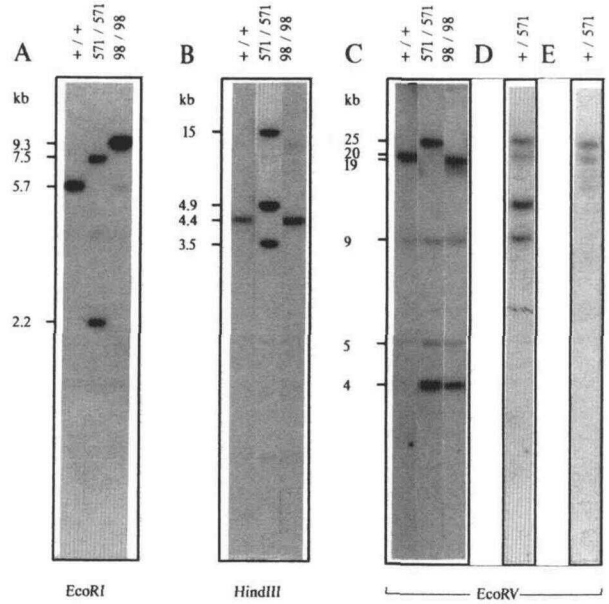

Figure 3. Gel Blot Hybridizations with 5 μg of *niv-571* Genomic DNA.

(A) Hybridization with the Am3 probe, a 5.7-kb EcoRI fragment of *Niv*$^+$.
(B) Hybridization with the END probe, a 0.57-kb EcoRI fragment from the right end of *Niv*$^+$.
(C) Probe as in **(A)**.
(D) Probe as in **(B)**.
(E) Hybridization with a probe comprising the 1.9-kb EcoRI fragment pJAM571A1 from the spacer between the α and β copies in *niv-571*. The origin of the probes is given in Figure 4.

The *niv-571* allele was cloned by screening with Am3, a genomic λEMBL4 library of EcoRI partially digested DNA of a *niv-571* homozygote. This yielded clone pJAM571A, which contained the 7.5-kb EcoRI fragment previously seen on DNA gel blots together with adjacent fragments. The restriction map of pJAM571A is shown in Figure 4A. The only apparent difference from the progenitor, *niv-98*, was a deletion starting from 3 bp within the right end of Tam3 and extending rightward to a position 1700 bp within the third exon of the *niv* gene, resulting in a truncated version of the *niv* gene, the α copy (Figure 4A). The numbering of nucleotides is relative to the *Niv*$^+$ transcription start site, as detailed by Sommer and Saedler (1986). At the newly generated junction (junction 1, Figure 4B), the hexanucleotide GGAGAA was inserted between Tam3 and the α copy. In pJAM571A, the restriction maps 3.8 kb upstream of Tam3 and 4.9 kb downstream of the α copy were identical to upstream and downstream maps in *niv-98*, *Niv*$^+$, and other *niv* alleles (Sommer and Saedler, 1986; C. Martin, personal communication). However, pJAM571A did not include the 2.2-kb EcoRI fragment observed in genomic DNA gel blot hybridizations of *niv-571* (Figure 3A). To clone the 2.2-kb EcoRI fragment, a size fraction of about 2.0 to 2.4 kb was gel purified from EcoRI-digested genomic DNA of *niv-571* homozygotes, cloned into the EcoRI site of λNM1149, and plaques were screened with Am3 to give the subclone pJAM571B. The sequences at both ends of the 2.2-kb insert were determined. For about 200 bp, both ends were identical to the sequence upstream of the EcoRI site in the third exon of the *Niv*$^+$ gene. Thus, pJAM571B contained two copies of the transcribed region of the *niv* gene, called the β and the γ copies, in opposite orientation relative to each other (Figure 4A).

To investigate whether the α, β, and γ copies of the *niv* locus also contained the 3′ end of the *niv* coding region (not included in the probe Am3), a 3′ probe of the *niv* gene was isolated. In the *Niv*$^+$ allele, a 0.57-kb EcoRI fragment containing 465 bp of the 3′ end of the *niv* gene and 110 bp of downstream sequences lies 3′ to the 5.7-kb Am3 fragment. This fragment is indicated as END in Figure 4A. In HindIII-digested DNA from *niv-571* homozygotes, three fragments (15, 4.9, and 3.5 kb) hybridized to this probe (Figure 3B). All three fragments cosegregated with the *niv-571* allele in F_2 populations (50 plants analyzed). The 15-kb fragment was thought to contain the α copy because this fragment was replaced by an 11.5-kb fragment in *niv-572*, an allele derived from *niv-571* by excision of Tam3 (see later). The 4.9-kb and the 3.5-kb HindIII fragments were cloned into the HindIII site of λNM1149, resulting in subclones pJAM571D and pJAM571E (Figure 3B). DNA gel blot hybridization showed them to overlap with pJAM571B and to extend further to the right or left, respectively.

pJAM571D, together with pJAM571B, allowed the γ copy to be characterized completely. It extended from within the third exon of the *Niv*$^+$ allele (position 1692, junction 3, Figure 4B) to the 3′ end of the transcribed region. Comparison of restriction maps and hybridizations showed that 3.3 kb of sequence downstream of the γ copy in pJAM571D was identical to the corresponding region of the *Niv*$^+$ allele.

pJAM571E, together with pJAM571B, allowed the β copy to be characterized. The β copy was an inverted copy of the *Niv*$^+$ allele from position −62 (junction 3, Figure 4B), which corresponds to a position 1 bp away from the Tam3 insertion site in *niv-98*, to position 2230 (junction 2, Figure 4B). Thus, the β copy was truncated, its end point lying within the third exon of the *niv* gene, 224 bp before the poly(A) addition sites. There was a new sequence to the left of the β copy, after position 2230. To test whether this new sequence was transcribed, a 1.4-kb SmaI-EcoRI fragment, pJAM571E1, containing 37 bp of the left end of the β copy and 1.35 kb of the new sequence extending leftward to the nearest EcoRI site, was used to probe RNA gel blots of flower RNA extracted from wild-type and *niv-571* plants; no hybridization signal was obtained.

The nucleotide sequence at the junction between the β and the γ copy (junction 3, Figure 4B) showed that the 10 bp to the right of the β copy were identical to the *Niv*$^+$

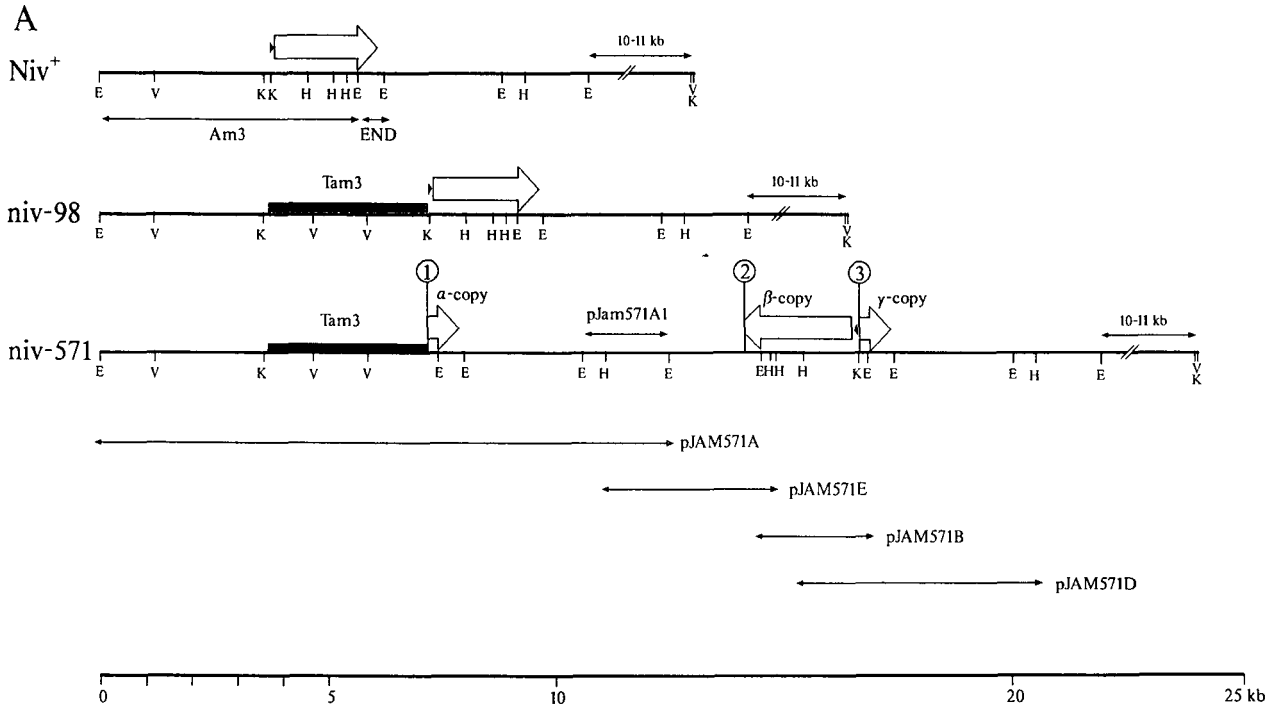

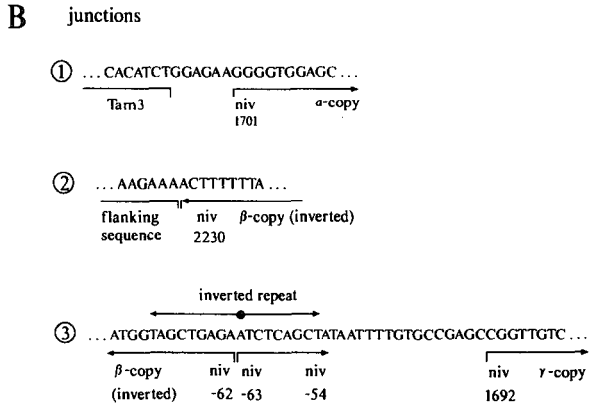

Figure 4. Structure of the Semidominant Allele *niv-571*.

(A) Restriction maps of *niv-571* and, for comparison, *niv-98* and *Niv*$^+$ (partly from Sommer and Saedler, 1986). Regions covered by genomic clones obtained are indicated below *niv-571*. Open arrows span sequences identical to the transcribed region in *Niv*$^+$; the solid bars indicate Tam3; the filled triangles mark the positions and orientations of sequences identical to the *Niv*$^+$ promoter sequence from position −63 to −1; α, β, and γ copies are marked; new junctions are numbered; fragments used as probes (Am3, pJAM571A1, and END) are indicated; the scale is given at the bottom.

(B) Nucleotide sequences (in 5′ to 3′ direction) at junctions 1, 2, and 3. The origins and orientations of sequence elements and the inverted repeat in junction 3 are indicated. End points of *niv* sequences are numbered according to Sommer and Saedler (1986).

promoter sequence from position −63 to position −54. Thus, there was a 9-bp inverted duplication of the region flanking Tam3 in the progenitor *niv-98*. Between this sequence and the γ copy (position 1692) was another 15 bp of sequence of unknown origin (Figure 4B).

The left end of pJAM571E also overlapped with the right end of clone pJAM571A, allowing the relative positions of the α, β, and γ copies to be mapped in a region covering 25 kb of the *niv-571* allele. With respect to upstream and downstream sequences, the α and γ copies were in normal orientation, and the β copy was inverted. The α and the β copies were 6.2 kb apart. As mentioned before, 4.9 kb of this spacer sequence, the region downstream of the α copy in pJAM571A, was identical to the sequence downstream of the *niv* gene in *Niv*$^+$ and *niv-98*. However, it was difficult to determine the origin of the remaining sequence immediately to the left of the β copy. The 1.4-kb SmaI-EcoRI fragment pJAM571E1, mentioned above, containing this sequence hybridized to at least 12 different fragments in genomic DNA from *niv-98*, preventing the cloning of its progenitor. However, it seemed likely that most, if not all, of this sequence was the normal downstream continuation of the *niv* locus.

To confirm the genomic organization of the *niv* locus, EcoRV-digested genomic DNA from wild-type, *niv-98*, and *niv-571* plants was probed with Am3 (Figure 3C). EcoRV cuts within Am3 and at corresponding positions in *niv-98* and in pJAM571A (Figure 4A). EcoRV fragments extending to the left of this site were expected to be identical for *Niv*$^+$ and *niv-98*. Because only about one-quarter of the

probe length should have hybridized to such fragments, the intensity of the signal was expected to be low compared to internal fragments or fragments extending to the right (see below). The only EcoRV fragments hybridizing in *Niv*$^+$ and *niv-98* with low intensities were 5 and 9 kb in length; one of these, therefore, should have corresponded to the sequence extending leftward. Because *niv-571* contained the same 5-kb and 9-kb fragments (Figure 3C), no major rearrangement had occurred upstream of the left EcoRV site in *niv-571* for at least 5 kb.

The strongly hybridizing 4-kb EcoRV fragments in *niv-98* and *niv-571* (Figure 3C) were internal fragments readily explained by the restriction maps in Figure 4A; they extended from the EcoRV site in Am3 to the first EcoRV site in Tam3 (Tam3 contains two EcoRV sites). As expected, because it lacked Tam3, *Niv*$^+$ did not have this fragment.

Differences were observed for EcoRV fragments extending to the right. Am3 hybridized to fragments of 20 kb in the wild type, 19 kb in *niv-98*, and 25 kb in *niv-571* (Figure 3C). The 20-kb wild-type fragment extended to the right from the only EcoRV site in the 5.7-kb Am3 fragment (Figure 4A). In *niv-571* and *niv-98*, the fragments extended rightward from the rightmost EcoRV site in Tam3. Within the overlapping clones of *niv-571*, there was no EcoRV site further to the right of Tam3, accounting for the large size of the EcoRV fragment. The fragments in *Niv*$^+$ and *niv-98* were both consistent with an EcoRV site lying about 18 kb to the right of the Tam3 insertion site. Because none of the overlapping clones of *niv-571* contained EcoRV sites, an EcoRV fragment about 6 kb longer than that observed in *niv-98* was expected, consistent with the 25-kb fragment seen. This confirmed that the sequence downstream of the γ copy in *niv-571* was identical to the region downstream of the *niv* gene in *Niv*$^+$. Further confirmation of this interpretation was obtained from analyzing KpnI digests probed with Am3 and END probes (data not shown).

Evidence for the structure of *niv-571* (Figure 4A) was also obtained when DNA from *Niv*$^+$*/niv-571* heterozygotes, cut with EcoRV, was probed with the 0.57-kb END fragment (Figure 3D), or with the subfragment pJAM571A1 (Figure 3E) from the spacer region between the α and the β copies (Figure 4B). The END probe hybridized two to three times more strongly to the 25-kb fragment (corresponding to *niv-571*) than to the 20-kb fragment (corresponding to the wild type), consistent with the 3′ end of the *niv* gene being triplicated. pJAM571A1 hybridized about twice as strongly to the 25-kb *niv-571* fragment than to the 20-kb wild-type fragment (Figure 3E), confirming that at least this part of the spacer region was duplicated.

Structure of *niv-572*

The Tam3 insertion in *niv-571* was unstable. In addition to the 2.2-kb and 7.5-kb EcoRI fragments, the 5.7-kb Am3 probe also hybridized weakly to a 3.9-kb EcoRI fragment, as shown in Figures 3A and 5A. This "weak" fragment might be explained by somatic excision of the 3.6-kb Tam3 element from the 7.5-kb fragment. In an attempt to obtain a germinal excision event, *niv-571* homozygotes were grown at 15°C, a temperature that favors Tam3 excision (Carpenter et al., 1987), and either self-pollinated or crossed to the wild type. Analysis of DNA from 13 plants of the subsequent generation showed that one plant had a 3.9-kb instead of a 7.5-kb fragment hybridizing to Am3. Similarly, in HindIII-digested genomic DNA, the 15-kb HindIII fragment typical of *niv-571* was replaced by a fragment of approximately 11 or 12 kb, as shown in Figure 5B. The differences in length suggested excision of Tam3 (3.6 kb). The presence of the 2.2-kb EcoRI fragment (Figure 5A), as well as the 3.5-kb and 4.9-kb HindIII fragments (Figure 5B), suggested that the β and γ copies were unaltered. This new *niv* allele, called *niv-572*, therefore appeared to differ from *niv-571* only in that Tam3 had been excised. To define this excision product more precisely, the 3.9-kb EcoRI fragment was cloned into λNM1149 (Figure 5C). Sequencing of junction 4 (Figure 5D) confirmed that Tam3 had been excised and that a deletion of 20 bp of the left flanking region had also occurred. The right flanking region was unaltered. *Niv*$^+$*/niv-572* heterozygotes were phenotypically indistinguishable from *Niv*$^+$*/niv-571* plants (Figure 1A); thus, excision of Tam3 did not affect the semidominance. Red sectors, often with diffuse boundaries, were occasionally seen on *Niv*$^+$*/niv-572* heterozygotes, similar to those previously described for *Niv*$^+$*/niv-571*.

Structure of *niv-527*

Many recessive *niv* alleles have been derived from *niv-98*. One of these, *niv-527* (Figure 1A), gave a null (white-flowered) phenotype and was selected for further molecular analysis. As seen in Figure 6A, this allele showed an EcoRI fragment of 3.9 kb when probed with Am3, a similar size to the EcoRI fragment that contained the α copy of *niv-572* (Figure 5A). Analysis of this allele, therefore, might have enabled the phenotypic effects of the α copy alone to be determined. The *niv-527* fragment was cloned in the EcoRI site of λNM1149, giving pJAM527 (Figure 6B), and characterized. Analysis of this plasmid showed that *niv-527* had resulted from an imprecise Tam3 excision that deleted 5 to 7 bp of the flanking sequence to the left and 1819 to 1821 bp to the right of the Tam3 excision site (junction 5, Figure 6C). The 3-bp sequence CAG at junction 5 could have been derived from either the left or the right flanking sequence, hence the ambiguity in the end points of the deletion. The 3.9-kb EcoRI fragment of *niv-527* thus differed from the fragment harboring the α copy of *niv-572* in having an extra 15 bp of *niv* promoter sequence (region −71 to −57) and lacking 57 bp from within the third exon of the *niv* coding sequence (region 1701 to 1757).

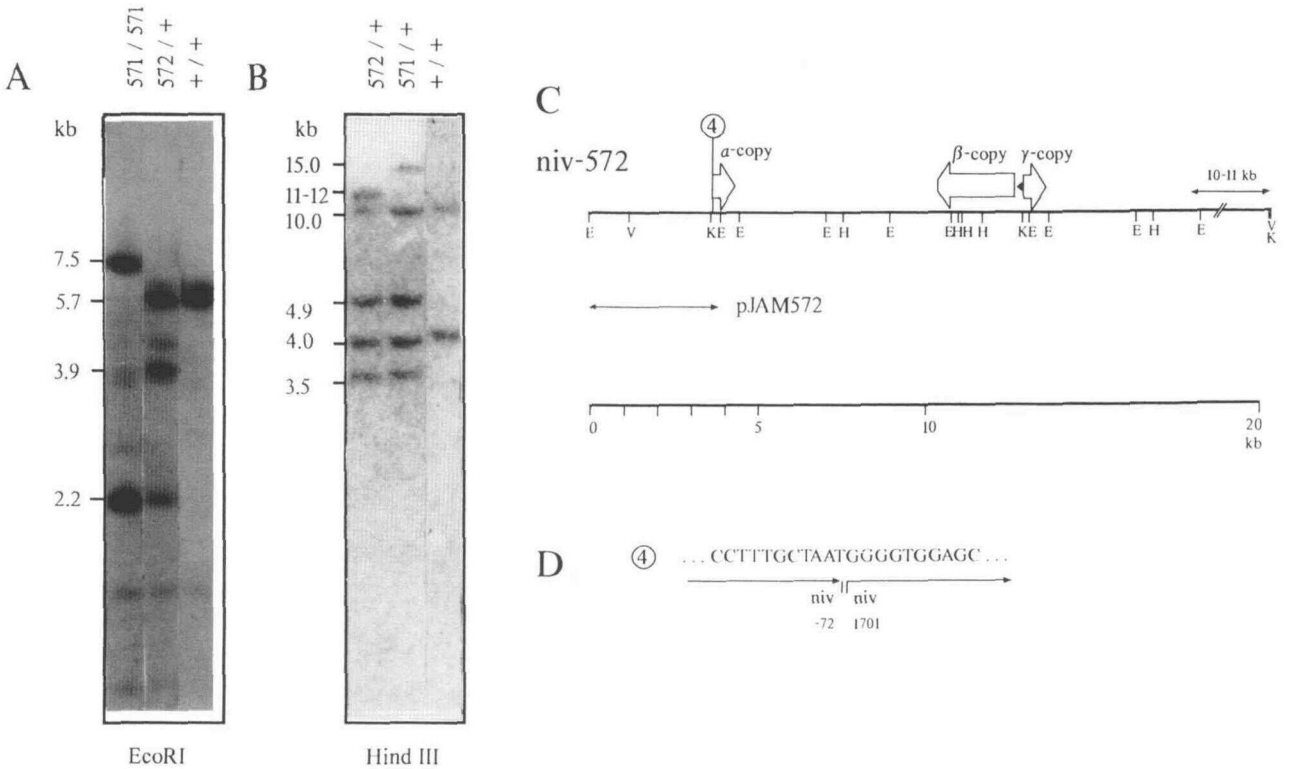

Figure 5. Molecular Organization of the Semidominant Allele *niv*-572.

(A) Gel blot hybridizations with genomic DNA. Am3 (see Figure 4A) was used as a probe.
(B) Gel blot hybridizations with genomic DNA. END (see Figure 4A) was used as a probe.
(C) Restriction map of *niv-572*. The region cloned in pJAM572 is indicated.
(D) Sequence at junction 4. Symbols are given in Figure 4.

DISCUSSION

When heterozygous with *Niv*$^+$, the *niv-571* allele acts in *trans* to reduce expression of the *Niv*$^+$ allele 25- to 50-fold. The *niv-571* allele has three truncated copies (called α, β, and γ) of the *niv* gene, one of which, the β copy, is inverted relative to the wild type. In addition, a duplication of the region 6 kb downstream of *niv* lies between the α and β copies, and a Tam3 insertion lies upstream of the α copy. Characterization of two further alleles, *niv-572* and *niv-527*, excludes several structural features of *niv-571* from being the cause of semidominance. Comparison of *niv-571*, which contains Tam3, and *niv-572*, its Tam3 excision product, excludes involvement of the transposon. Similarly, the almost identical molecular structures of the recessive *niv-527* allele and the α copy of *niv-572* exclude the α copy alone from being responsible. Comparison of *niv-571* and *572* with recessive alleles and with a previously described but less phenotypically extreme semidominant allele, *niv-525*, shows that all semidominant *niv* alleles have inversions and multiple copies of *niv* gene sequences. How could these structural features account for the semidominance of these alleles?

One possibility is that the semidominant alleles might produce antisense RNA by transcription of the inverted regions of the *niv* gene. In *niv-525*, antisense RNA production might be driven by the normal *niv* promoter to produce a transcript complementary to part of the *niv* wild-type transcript (Coen and Carpenter, 1988). Similarly, in *niv-571* and *572*, a promoter within the spacer sequence (region B), as shown in Figure 7, might drive transcription into the inverted β copy. However, several features are not easily reconciled with the involvement of antisense RNA.

(1) The spatial patterns of expression of antisense RNA might be expected to be different for *niv-571* and *572* compared with *niv-525* because antisense RNA production would be driven by two different promoters. However, the spatial pattern of flower coloration of *Niv*$^+$/*niv-571* plants is very similar to that of *niv-525*/*niv-525* and *Niv*$^+$/*niv-525* plants (Figure 1A). This type of pattern seems to be diagnostic of semidominant *niv* alleles because so far it has not been observed in recessive *niv* mutants. It is

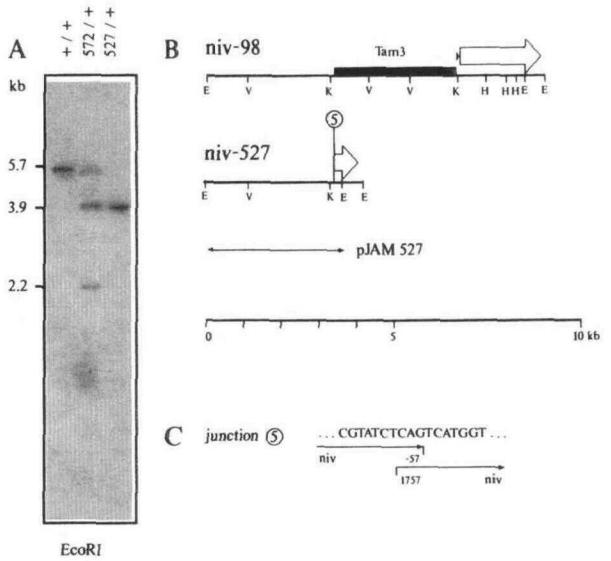

Figure 6. Molecular Organization of the Recessive Allele *niv-527*.

(A) Gel blot hybridization with genomic DNA digested with EcoRI. Am3 was used as a probe.
(B) Restriction maps of *niv-527* and, for comparison, *niv-98*. The region cloned in pJAM527 is indicated.
(C) Sequence at junction 5. Symbols are given in Figure 4.

unlikely that two different promoters would show exactly the same spatial expression pattern. A modified explanation, assuming that in *niv-571* and *572* transcription is driven by the normal *niv* promoter starting with the α copy and running into the inverted β copy, is most unlikely because the normal *niv* TATA box is missing in these alleles.

(2) RNA gel blot hybridizations using DNA labeled in both strands by nick translation (this paper) or S1 protection assays (Coen and Carpenter, 1988) failed to detect any transcript other than the wild-type transcript in heterozygous plants carrying semidominant alleles, even though large amounts of antisense RNA (at least 49% of homozygous wild type) would be necessary to result in the 50-fold reduction of *Niv*$^+$ expression observed. It is possible, however, that antisense RNA could have evaded detection by these methods if it were localized exclusively in the nucleus or if it had a relatively short half-life.

(3) If a promoter located at some distance to the left of the β copy were responsible for producing an antisense RNA, then a transcript resulting from the activity of this promoter should be detectable in *Niv*$^+$ plants. However, we did not detect transcripts using a fragment comprising the right end of the spacer region as a probe. We conclude, therefore, that the antisense RNA model does not easily account for the semidominance of these *niv* alleles.

A more likely explanation for the semidominance is that it reflects physical recognition and interaction between alleles. This type of model has been proposed to account for some transvection phenomena in Drosophila, in which a protein encoded by the *zeste* locus is thought to mediate interactions between synapsed alleles (Bickel and Pirrotta, 1990). Recognition between related sequences also has been proposed to account for gene interaction associated with the presence of multiple gene copies, namely cosuppression in plants (for review, see Jorgensen, 1990) and repeat-induced point mutations (RIP), or RIP-related phenomena, in fungi (Faugeron et al., 1990; Selker, 1990). In the case of cosuppression, for example, introduction of an extra copy of a chalcone synthase gene (the same enzyme as that encoded by *niv*) in the petunia genome can result in inhibition of the endogenous chalcone synthase gene, giving white-flowered plants (Napoli et al., 1990; van der Krol et al., 1990). Unlike transvection, cosuppression and RIP do not require the interacting genes to be at homologous chromosomal positions, although it is not known whether this reflects a qualitative difference in the underlying mechanisms or a difference in the efficiency of gene recognition/interaction in the two systems. A further important feature of both cosuppression and transvection is that they are fully reversible following meiosis so that the wild-type gene reverts to its normal expression pattern as soon as it segregates away from the inhibiting gene. This is not true of the RIP phenomenon

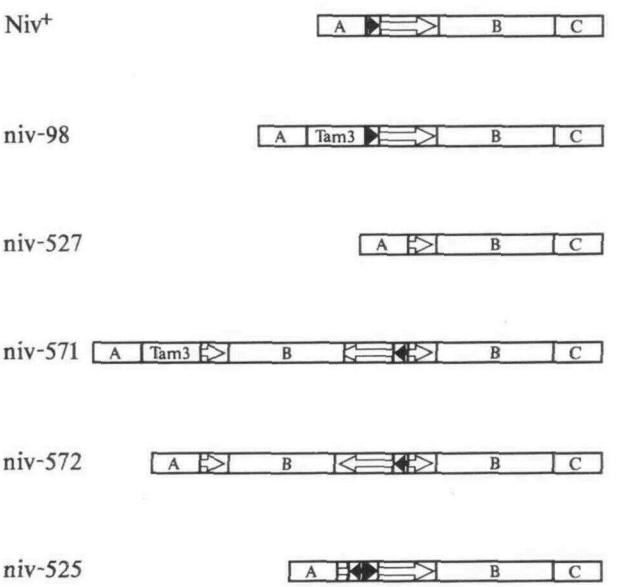

Figure 7. Structural Comparison of *niv* Alleles of Antirrhinum.

The filled arrowheads mark the positions and orientations of sequences identical to the *Niv*$^+$ promoter sequence from position −63 to −1. The open arrows indicate sequences identical to the transcribed region in *Niv*$^+$; A, upstream sequences; B, sequences identical to the spacer between the α and β copies in *niv-571/2*; C, downstream sequences. This figure is not drawn to scale.

in Neurospora, where the inactivated state of a gene may be heritable (Selker, 1990). It is possible, however, that such differences between systems reflect alternative ways in which repression is maintained following a common initial mechanism of recognition/interaction.

Several structural features of the semidominant *niv* alleles might provide the basis of recognition/interaction with Niv^+. All semidominant alleles have an inversion of *niv* sequences including a particular region of the promoter/leader sequence in common. It is possible that this inverted copy might specifically interact with the normally oriented wild-type homolog, either directly or by way of protein-DNA interactions. Alternatively, the semidominance might depend on the overall features of inverted or direct duplications, perhaps analogous to the properties of ectopic gene copies involved in cosuppression (Jorgensen, 1990). Unfortunately, it is not known whether the *trans* effect of the semidominant *niv* alleles depends on the affected Niv^+ allele being at a homologous chromosomal position (a requirement of transvection) or whether it could also occur if the inhibiting allele were at a different chromosomal location in the genome (as observed in cosuppression).

One further important feature of the semidominant *niv* alleles is that repression of Niv^+ is fully reversible. Following meiosis, no stable heritable alteration of Niv^+ occurs; thus, if epigenetic changes such as methylation are involved, they would have to be erased following meiotic segregation. Similarly, evidence for somatic reversibility is provided by the partial restoration of *niv* expression occasionally observed in *niv-571*/Niv^+ heterozygotes (Figures 1B and 1C). Somatic instability also has been observed for cosuppression in petunia (Linn et al., 1990; Napoli et al., 1990; van der Krol et al., 1990). The somatic reversions in *niv-571*/Niv^+ heterozygotes are unlikely to be solely a consequence of the Tam3 insertion in *niv-571* because similar reversions are also observed when Niv^+ is heterozygous with *niv-572*, which lacks Tam3. Another mechanism of somatic mutation is presumably involved. The diffuse boundaries of some red sectors suggest that restoration of *niv* activity is not fully cell autonomous (Figure 1C). This is puzzling because transposon-induced clonal mutations at the *niv* locus result in sharp boundaries between sectors, indicating that *niv* acts in a cell autonomous manner. It should be noted, however, that even when somatic reversion affects a complete flower, pigmented and pale regions of the flower are separated by zones of intermediate intensity. It is difficult, therefore, in some cases to clearly separate diffuseness resulting from nonautonomy from that due to various patterns that can arise by somatic reversion. Similar diffuse sectors have also been observed in some cases of cosuppression in petunia (Jorgensen, 1990; Napoli et al., 1990).

From these considerations, the action of semidominant *niv* alleles probably depends on a mechanism that allows related sequences to recognize and interact with each other and, hence, modify their expression patterns. A similar process may underlie related phenomena described in other systems; the distinct features of each system may reflect differences in the constraints on how recognition is established and altered expression maintained.

Origin of the *niv* Alleles

niv-571 was derived from *niv-98*, which contains an active copy of Tam3 inserted in the promoter region. A combination of several different processes, including generation of inverted duplications, deletions, and translocation between chromatids, may be invoked to explain its origin. Because intermediate structures have not been obtained, however, the precise order of these processes is unknown. The generation of *niv-572* from *niv-571* and of *niv-527* from *niv-98* is readily explained according to current models of transposition by Tam3 excision events with concomitant removal of flanking sequences (Saedler and Nevers, 1985; Coen et al., 1989).

Small sequence elements at newly generated junctions (Figure 4B) are of uncertain provenance, except for the 9-bp inverted duplication at junction 3, which appears to be a remnant of a hairpin loop presumably formed during transposition. Nucleotide sequences similar to parts of this junction sequence are also found in the parts of the *niv* sequence that presumably have been deleted during *niv-571* formation. For example, the sequence AATTTTGTG in junction 3 is identical to position 1447 to 1455 of the *niv* gene and most likely derived from it. Martin and Lister (1989) and Martin et al. (1988), who studied rather complex rearrangements at the *niv* locus, and Almeida et al. (1989) also found small strings of sequences at newly generated junctions. Breakdown products generated during deletion may perhaps have been fortuitously picked up by newly formed junctions.

METHODS

Plant Stocks

niv alleles have the same numbers as the lines of *Antirrhinum majus* in which they are maintained. Niv^+, *niv-98*, and *niv-525* were described previously (Sommer and Saedler, 1986; Carpenter et al., 1987; Coen and Carpenter, 1988).

Molecular Analysis

The method for anthocyanin extraction and quantification was detailed previously (Coen et al., 1986). Standard molecular genetic analysis was conducted as described by Maniatis et al. (1982). The chalcone synthase probe for RNA gel blot hybridizations was the cDNA clone pAm10 (Sommer and Saedler, 1986), and the *pallida* probe was a 4.3-kb HindIII fragment from pJAM501 (Coen et al., 1986). RNA was extracted from flowers according to Martin and Northcote (1981). Gel-purified genomic DNA was cloned into λEMBL4 (Frischauf et al., 1983) or λNM1149 (Murray, 1982).

Hybridization was at 65°C in 3 × SSC (1 × SSC is 0.15 M NaCl, 0.015 M sodium citrate), 0.1% SDS, 0.02% Ficoll, 0.02% polyvinylpyrrolidone. Restriction digests (with the exception of KpnI digests) were done in the presence of 5 mM spermidine. The dideoxy sequencing method was used according to Sanger et al. (1977).

ACKNOWLEDGMENTS

We would like to thank Hans Sommer for providing chalcone synthase clones, Peter Scott and Andrew Davies for photography, and Rich Jorgensen for helpful comments on the manuscript. J.B. was supported by a grant within the Biotechnology Action Program of the European Community.

Received August 23, 1991; accepted October 28, 1991.

REFERENCES

Almeida, J., Carpenter, R., Robbins, T.P., Martin, C., and Coen, E.S. (1989). Genetic interactions underlying flower color patterns in *Antirrhinum majus*. Genes Dev. **3,** 1758–1767.

Bickel, S., and Pirrotta, V. (1990). Self-association of the Drosophila *zeste* protein is responsible for transvection effects. EMBO J. **9,** 2959–2967.

Carpenter, R., Martin, C.R., and Coen, E.S. (1987). Comparison of genetic behaviour of the transposable element Tam3 at two unlinked pigment loci in *Antirrhinum majus*. Mol. Gen. Genet. **207,** 82–89.

Coen, E.S., and Carpenter, R. (1988). A semidominant allele, *niv-525*, acts *in trans* to inhibit expression of its wild-type homologue in *Antirrhinum majus*. EMBO J. **7,** 877–883.

Coen, E.S., Carpenter, R., and Martin, C. (1986). Transposable elements generate novel spatial patterns of gene expression in *Antirrhinum majus*. Cell **47,** 285–296.

Coen, E.S., Robbins, T.P., Almeida, J., Hudson, A., and Carpenter, R. (1989). Consequences and mechanisms of transposition in *Antirrhinum majus*. In Mobile DNA, D. Berg and M. Howe, eds (Washington, DC: American Society for Microbiology), pp. 413–436.

Davies, K. (1991). The essence of inactivity. Nature **349,** 15–16.

Faugeron, G., Rhounim, L., and Rossignol, J.-L. (1990). How does the cell count the number of ectopic copies of a gene in the premeiotic inactivation process acting in *Ascobolus immersus*? Genetics **124,** 585–591.

Frischauf, A.-M., Lehrach, H., Poustka, A., and Murray, N. (1983). λ replacement vectors carrying polylinker sequences. J. Mol. Biol. **170,** 827–842.

Geyer, P.K., Green, M.M., and Corces, V.G. (1990). Tissue-specific transcriptional enhancers may act *in trans* on the gene located in the homologous chromosome: The molecular basis of transvection in Drosophila. EMBO J. **9,** 2247–2256.

Jorgensen, R. (1990). Altered gene expression in plants due to *trans* interactions between homologous genes. Tibtech. **8,** 340–344.

Linn, F., Heidmann, I., Saedler, H., and Meyer, P. (1990). Epigenetic changes in the expression of the maize A1 gene in *Petunia hybrida*: Role of numbers of integrated gene copies and state of methylation. Mol. Gen. Genet. **222,** 329–336.

Maniatis, T., Fritsch, E.F., and Sambrook, J. (1982). Molecular Cloning. A Laboratory Manual. (Cold Spring Harbor, NY: Cold Spring Harbor Laboratory).

Martin, C., and Lister, C. (1989). Genome juggling by transposons: Tam3-induced rearrangements in *Antirrhinum majus*. Dev. Genet. **10,** 438–451.

Martin, C., and Northcote, D.H. (1981). Qualitative and quantitative changes in mRNA of castor beans during initial stages of germination. Planta **151,** 189–197.

Martin, C., MacKay, S., and Carpenter, R. (1988). Large-scale chromosomal restructuring is induced by the transposable element Tam3 at the *nivea* locus of *Antirrhinum majus*. Genetics **119,** 171–184.

Murray, N.E. (1982). Phage lambda and molecular cloning. In Lambda II, R.W. Hendrix, J.W. Roberts, F.W. Stahl, and R.A. Weissberg, eds (Cold Spring Harbor, NY: Cold Spring Harbor Laboratory), pp. 395–442.

Napoli, C., Lemieux, C., and Jorgensen, R. (1990). Introduction of a chimeric chalcone synthase gene into petunia results in reversible co-suppression of homologous genes *in trans*. Plant Cell **2,** 279–289.

Saedler, H., and Nevers, P. (1985). Transposition in plants: A molecular model. EMBO J. **4,** 585–590.

Sanger, F., Nicklen, S., and Coulson, A.R. (1977). DNA sequencing with chain terminating inhibitors. Proc. Natl. Acad. Sci. USA **74,** 5463–5467.

Selker, E.U. (1990). Premeiotic instability of repeated sequences in *Neurospora crassa*. Annu. Rev. Genet. **24,** 579–613.

Sommer, H., and Saedler, H. (1986). Structure of the chalcone synthase gene of *Antirrhinum majus*. Mol. Gen. Genet. **202,** 429–434.

Sommer, H., Carpenter, R., Harrison, B.J., and Saedler, H. (1985). The transposable element Tam3 of *Antirrhinum majus* generates a novel type of sequence alteration upon excision. Mol. Gen. Genet. **199,** 225–231.

Sommer, H., Bonas, U., and Saedler, H. (1988). Transposon-induced alterations in the promoter region affect transcription of the chalcone synthase gene in *Antirrhinum majus*. Mol. Gen. Genet. **211,** 49–55.

Wu, C.-T., and Goldberg, M.L. (1989). The Drosophila *zeste* gene and transvection. Trends Genet. **5,** 189–194.

van der Krol, A.R., Mur, L.A., Beld, M., Mol, J.N.M., and Stuitje, A.R. (1990). Flavonoid genes in petunia: Addition of a limited number of gene copies may lead to a suppression of gene expression. Plant Cell **2,** 291–299.